Physica B 481 (2016) 91–96

Contents lists available at ScienceDirect

Physica B

journal homepage: www.elsevier.com/locate/physb

Room temperature ferromagnetism in Mn doped ZnO: Co nanoparticles by co-precipitation method

V. Pazhanivelu [a], A. Paul Blessington Selvadurai [a], Yongsheng Zhao [b], R. Thiyagarajan [b], R. Murugaraj [a,*]

[a] Department of Physics, Anna University, Chennai 600044, India
[b] Center for High Pressure Science and Technology Advanced Research, 1690 Cailun Road, Shanghai 201203, China

ARTICLE INFO

Article history:
Received 19 September 2015
Received in revised form
20 October 2015
Accepted 23 October 2015
Available online 28 October 2015

Keywords:
Doped ZnO
Nanoparticles
Phololuminscence
Electron paramagnetic resonance
Zn interstitial defects
RTFM

ABSTRACT

In this present work, the Mn^{2+} and Co^{2+} ions doping and co-doping effect on the structural, vibrational, morphological, optical and magnetic behaviors of ZnO based dilute magnetic semiconductors are reported. The $Zn_{0.95}Co_{0.05}O$ (ZC), $Zn_{0.95}Mn_{0.05}O$ (ZM) and $Zn_{0.90}Co_{0.05}Mn_{0.05}O$ (ZCM) samples were prepared by co-precipitation method. From the XRD analysis, it was observed that on the doping of Mn^{2+} ion in ZnO matrix, decreases their crystalline nature as well as the crystallite size significantly. The Raman spectra, Photoluminescence and electron paramagnetic resonance spectroscopy measurements reveal that the presence of defects in prepared samples. The UV-DRS spectroscopic exhibits the incorporation of dopant ions and their effect on the band gap subsequently. The magnetization measurements suggest the room temperature ferromagnetism (RTFM) in the prepared samples. The observed RTFM phenomenon was discussed based on the defects and grain confinement.

1. Introduction

Dilute Magnetic Semiconductors (DMSs) have attracted great interest in the recent years, because of their state-of- the art applications in the field of modern information technology through the spintronics devices. Also, they have been widely used in multifunctional fields such as optical, optoelectronic, varsistor and gas sensing, etc. [1]. In particular, ZnO is one of the prototypical metal oxide semiconductors having a wide band gap (3.327 eV) and large exciton binding energy (60 meV). Generally, one may expect that the perturbations such as impurity doping and/or sintering can change the basic characteristics of the physical systems through by altering their electronic configurations. In ZnO based DMS materials, a low concentration impurity doping and sintering environment also affects its physical properties. Earlier, Dietl et al., reported that the existence of RTFM with a *p*-type semiconducting properties in Mn-doped ZnO system [2]. However, the doping of other transition-metal (TM) ions such as Cr [3], Mn [4,5], Fe [6], Ni [7], Co [8–10] and Cu [11] also shows RTFM behavior irrespective of physical forms such as powders and/or thin films. Particularly, the co-doping of Alkali [12], Alkaline metal ions [13] and rare-earth ions (RE) [14] with TM: ZnO powders have been widely studied both theoretically and experimentally by various research groups around the world.

So far, various preparation methods such as sputtering, spray-pyrolysis, Metal–Organic Chemical Vapor Deposition (MOCVD) and Pulsed Laser Deposition (PLD) were reported for co-doping of Mn ions in doped ZnO thin films [15–24]. Apart from thin film formations, there were some reports on bulk form of Mn codoped ZnO:Co nanomaterials with different reasoning for the presence of RTFM. Out of them, a few reports are as follows: The Li^{+} co-doped and Li^{3+} ions irradiate ZnO:Mn powders prepared by co-precipitation and solid state reaction method, respectively. Both the systems exhibit RTFM due to their Zn vacancy defects [25,26]. However, the Mn codoped with Fe and Cr ions prepared by solid state reaction and hydrothermal method respectively, explained the RTFM behavior through bounded magnetic polarons (BMP) exchange interactions [27,28]. Kai-Cheng Zhang et al., theoretically predicted that the suppression of the AFM exchange interaction and enhancement of RTFM in ZnO:Mn system through the hole-mediated double-exchange interactions [29]. But, Duan et al., prepared Mn–Co codoped ZnO powders by auto-combustion method and the presence of lattice defects is a reason for RTFM in this system [30].

Similarly, Hengda Li et al., reported that the doping concentration of Mn plays a crucial role in RTFM of Mn co-doped ZnO: Co nanoparticles prepared by the sol–gel method. According to the

* Corresponding author.
E-mail address: r.murugaraj@gmail.com (R. Murugaraj).

http://dx.doi.org/10.1016/j.physb.2015.10.024
0921-4526/

RKKY theory, the doping concentration of Mn increases the delocalized carrier concentrations in the sample. Subsequently, the exchange interactions between the delocalized carriers and the conduction band electrons were led to RTFM behavior [31]. Sabiu et al., reported that $Zn_{0.9-x}Co_{0.1}Mn_xO$ exhibits RTFM by lattice defects such as Zn interstitial and O vacancies upto $x=0.2$ [32]. According to previous reports, the different preparation methods for TM doped ZnO nanomaterials and suggested the various phenomena for the existence of RTFM. In general, the doping element induces the lattice defects and alters the carrier concentrations in the ZnO doped sample. Till now, the mechanism behind RTFM was claimed by exchange interactions such as double-exchange, super-exchange and dopant electrons-delocalized conduction band electron interactions. The dopant related secondary phase formations, magnetic clusters and metal precipitations were played a vital role in the magnetic behavior of doped ZnO systems. Hence, the origin of RTFM is still not completely relieved, and open up a new window in spintronics materials research.

By keeping these points in mind, we aim to investigate the doping effect of Co, Mn and co-doping of Co, Mn ions in ZnO nanoparticles through standardized procedures. Even though there are so many reports on the same compositions, we do again the same for comparing our results with different sample forms and preparation techniques.

2. Experimental

The $Zn_{0.95}Co_{0.05}O$ (ZC), $Zn_{0.95}Mn_{0.05}O$ (ZM) and $Zn_{0.90}Co_{0.05}Mn_{0.05}O$ (ZCM) nanoparticle samples were prepared by co-precipitation method with precursors such as zinc acetate [Zn $(CH_3COO)_2 \cdot H_2O$], cobalt acetate [Co $(CH_3COO)_2 \cdot 4H_2O$], [Mn $(CH_3COO)_2 \cdot 4H_2O$] and oxalic acid [$(COOH)_2 \cdot 2H_2O$] as starting materials [10]. The crystalline nature of the samples was confirmed by the powder XRD patterns using Bruker D2 Phaser X-Ray Diffractometer. The surface morphology was characterized by Scanning Electronic Microscopy (SEM; FEI Quanta FEG 200 model). The Raman scattering spectral measurements were carried out for the prepared samples using Renishaw inVia Reflex system with 0.6 mW power of Ar^+ ion laser with excitation wavelength of 488 nm at room temperature. The UV Diffuse Reflectance Spectroscopy (DRS) (Shimadzu UV 2450 PC spectrophotometer) and Photoluminescence (JY Fluorolog-3 spectroflourometer) studies was carried out to investigate the optical and emission properties of the samples respectively. The EPR measurements were performed on a JEOL-JES FA200 spectrometer at room temperature on powdered samples. The magnetic property of all the samples at room temperature was analyzed through the magnetic field dependence of magnetization measurements using Lakeshore-7404 vibrating sample magnetometer.

3. Results

3.1. Structural properties

The powder XRD pattern for all the samples have been employed with Cu-K_α ($\lambda=1.542$ Å) radiation at a constant slow scanning rate of 0.20 s^{-1} and are shown in Fig. 1(a). The observed XRD patterns confirmed that all compositions are found to be in a single phase. They are also in good agreement with the standard pattern of pure ZnO [JCPDS no. 76-0704] at room temperature and belonging to the hexagonal Wurtizite structure. Compared with ZC sample, the peak positions of XRD patterns for doped compounds such as ZM and ZCM shifts towards the higher angle slightly. However, the intensity of the diffraction peaks is decreased appreciably. This is attributed due to the decreasing of the grain size

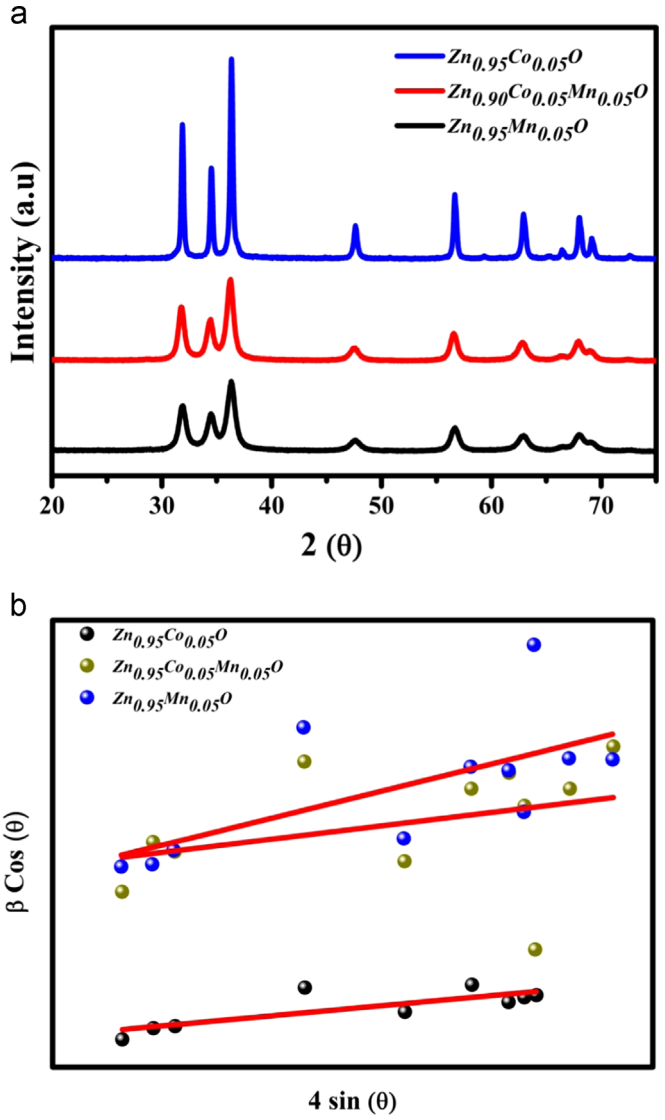

Fig. 1. (a) XRD pattern of ZC, ZM and ZCM samples; (b) W–H plot of ZC, ZM and ZCM samples.

by the doping of Mn in ZC sample.

From the XRD data, a few general parameters such as crystalline size, Lattice parameters, volumes and bond lengths were estimated as follows: The crystalline sizes were calculated by both the standard Scherrer's equation $\frac{0.94\lambda}{\beta \cos\theta}$ and Williamson–Hall (W–H) method. The lattice parameters such as a and c were calculated using a standard formula

$$\frac{1}{d_{hkl}^2} = \frac{4}{3}\left[\frac{h^2+hk+k^2}{a^2}\right] + \frac{l^2}{c^2}.$$

Subsequently, the unit cell volume was also estimated [33]. Finally, the bond length between Zn and O has been calculated using the following relation

$$e = \sqrt{\left(\frac{a^2}{3} + \left(\frac{1}{2}-u\right)^2 c^2\right)}$$

where u as a potential parameters of the structure [33]. Fig. 1 (b) shows the $4\sin\theta$ *vs* $\beta\cos\theta$ plots for calculating the lattice strain for the three samples. All these calculated parameters for the three samples were summarized in Table 1. From Table 1, it is observed that the crystalline sizes of all three samples estimated